Escherichia coli Cystathionine γ-Synthase Does Not Obey Ping-Pong Kinetics. Novel Continuous Assays for the Elimination and Substitution Reactions[†]

Susan M. Aitken, Daniel H. Kim, and Jack F. Kirsch*

Molecular and Cell Biology Department, University of California—Berkeley, Berkeley, California 94720-3206

Received June 27, 2003

ABSTRACT: Cystathionine γ-synthase (CGS) is a pyridoxal phosphate-dependent enzyme that catalyzes a γ-replacement reaction, in which the succinyl group of an *O*-succinyl-L-homoserine (L-OSHS) is displaced by the thiol of L-cysteine to form L-cystathionine, in the first step of the bacterial transsulfuration pathway. The mechanism of *Escherichia coli* CGS (eCGS) is ordered with L-OSHS associating before L-Cys ($k_{catR}/K_{mR}^{L-OSHS} = 9.8 \times 10^4\ M^{-1}\ s^{-1}$, where the subscript R denotes the replacement reaction). The mechanism becomes ping-pong ($k_{catR}/K_{mR}^{L-OSHS} = 4.9 \times 10^4\ M^{-1}\ s^{-1}$) at L-Cys concentrations lower than K_m^{L-Cys}. The enzyme also catalyzes a competing γ-elimination reaction, in which L-OSHS is hydrolyzed to succinate, NH_3, and α-ketobutyrate ($k_{catE}/K_{mE}^{L-OSHS} = 1350 \pm 90\ M^{-1}\ s^{-1}$, where the subscript E denotes the elimination reaction). The k_{cat}/K_m^{L-OSHS} *versus* pH profile of eCGS is bell-shaped for both reactions. The pH optimum and the pK_a values for the acidic and basic limbs are 7.4, 6.8 ± 0.1, and 8.0 ± 0.1, respectively, for the elimination reaction and 7.8, 7.4 ± 0.1, and 8.3 ± 0.1, respectively, for the replacement reaction. The internal aldimine of eCGS remains protonated at pH <10.5, and the α-amino group of L-OSHS has a pK_a of 9.71 ± 0.01; therefore, neither limb of the k_{cat}/K_m^{L-OSHS} *versus* pH profiles can be assigned to aldimine, or to L-OSHS prototropy. Novel continuous assays for the elimination reaction, employing D-2-hydroxyisocaproate dehydrogenase, and for the substitution reaction, employing cystathionine β-lyase and L-lactate dehydrogenase as coupling enzymes, are described.

Cystathionine γ-synthase (CGS)[1] catalyzes a γ-replacement reaction (Scheme 1) in which the leaving group of an activated form of L-homoserine is exchanged for the thiol of cysteine (L-Cys) to form L-cystathionine (L-Cth). This reaction is the first in the transsulfuration pathway that converts L-Cys to L-homocysteine (L-Hcys), the immediate precursor to L-methionine (Scheme 2). CGS and the subsequent enzyme in the pathway, cystathionine β-lyase (CBL), are unique to plants and bacteria and are therefore of interest as potential targets for antibiotics and herbicides (*1*). *O*-Succinyl-L-homoserine (L-OSHS), *O*-acetyl-L-homoserine, and *O*-phospho-L-homoserine are substrates for CGS from bacteria, fungi, and plants, respectively (*2*−*4*).

CGS is a homotetramer in which the active site, located at the subunit interface of the catalytic dimer, is comprised of residues from each subunit (*1*, *5*). *Escherichia coli* CGS (eCGS) is ∼30, 32, and 38% identical in sequence to CGS from other species, *E. coli* CBL (eCBL), and cystathionine γ-lyase from yeast (yCGL), respectively. eCGS is also similar in structure to these related enzymes (*1*, *6*). The rms deviation is only ∼1.5 Å between ∼350 C_α atoms in the least-squares superposition of eCGS on eCBL and yCGL (*1*, *6*).

The unique γ-replacement mechanism of CGS has attracted attention since the 1960s. Most studies have focused on the *Salmonella typhimurium* enzyme [stCGS (*7*−*10*)], but eCGS has also been investigated (*11*, *12*). Although the formation of L-Cth via the γ-replacement reaction is the only physiologically relevant reaction of CGS, both eCGS and stCGS also catalyze a γ-elimination reaction (Scheme 3), in which L-OSHS is hydrolyzed to succinate, NH_3, and α-ketobutyrate (α-KB) (*12*, *13*). The γ-elimination of succinate from L-OSHS is common to both the replacement and elimination reactions (Schemes 1 and 3), and a β,γ-unsaturated ketimine has been identified as the partitioning intermediate between these reactions (*12*).

The crystal structure (*1*) and the identity of the ketimine partitioning intermediate (*12*) of eCGS provide valuable

[†] This work was supported by NIH Grant GM35393. S.M.A. was supported by a postdoctoral research fellowship from the Natural Sciences and Engineering Research Council of Canada.

* To whom correspondence should be addressed. Telephone: (510) 642-6368. Fax: (510) 642-6368. E-mail: jfkirsch@uclink.berkeley.edu.

[1] Abbreviations: AATase, aspartate aminotransferase; AMPSO, *N*-(1,1-dimethyl-2-hydroxyethyl)-3-amino-2-hydroxypropanesulfonic acid; CAPS, 3-(cyclohexylamino)-1-propanesulfonic acid; CBL, cystathionine β-lyase; eCBL, *E. coli* cystathionine β-lyase; yCBS, yeast cystathionine β-synthase; CGL, cystathionine γ-lyase; CGS, cystathionine γ-synthase; eCGS, *E. coli* CGS; stCGS, *S. typhimurium* CGS; L-Cth, L-cystathionine; DTNB, 5,5′-dithiobis(2-nitrobenzoic acid); EDTA, ethylenediaminetetraacetic acid; L-Hcys, L-homocysteine; HO-HxoDH, D-2-hydroxyisocaproate dehydrogenase; IPTG, isopropyl β-D-thiogalactopyranoside; α-KB, α-ketobutyrate; LDH, L-lactate dehydrogenase; MBP, three-component buffer comprised of 50 mM MOPS, 50 mM Bicine, and 50 mM proline; MOPS, 3-(*N*-morpholino)propanesulfonic acid; NADH, β-nicotinamide adenine dinucleotide (reduced form); $NaPP_i$, sodium pyrophosphate; L-OSHS, *O*-succinyl-L-homoserine; PCR, polymerase chain reaction; PLP, pyridoxal 5′-phosphate; TAPS, *N*-[tris(hydroxymethyl)methyl]-3-aminopropanesulfonic acid.

10.1021/bi035107o CCC: $25.00
Published on Web 08/30/2003

Scheme 1: Mechanism of the eCGS γ-Replacement Reaction[a]

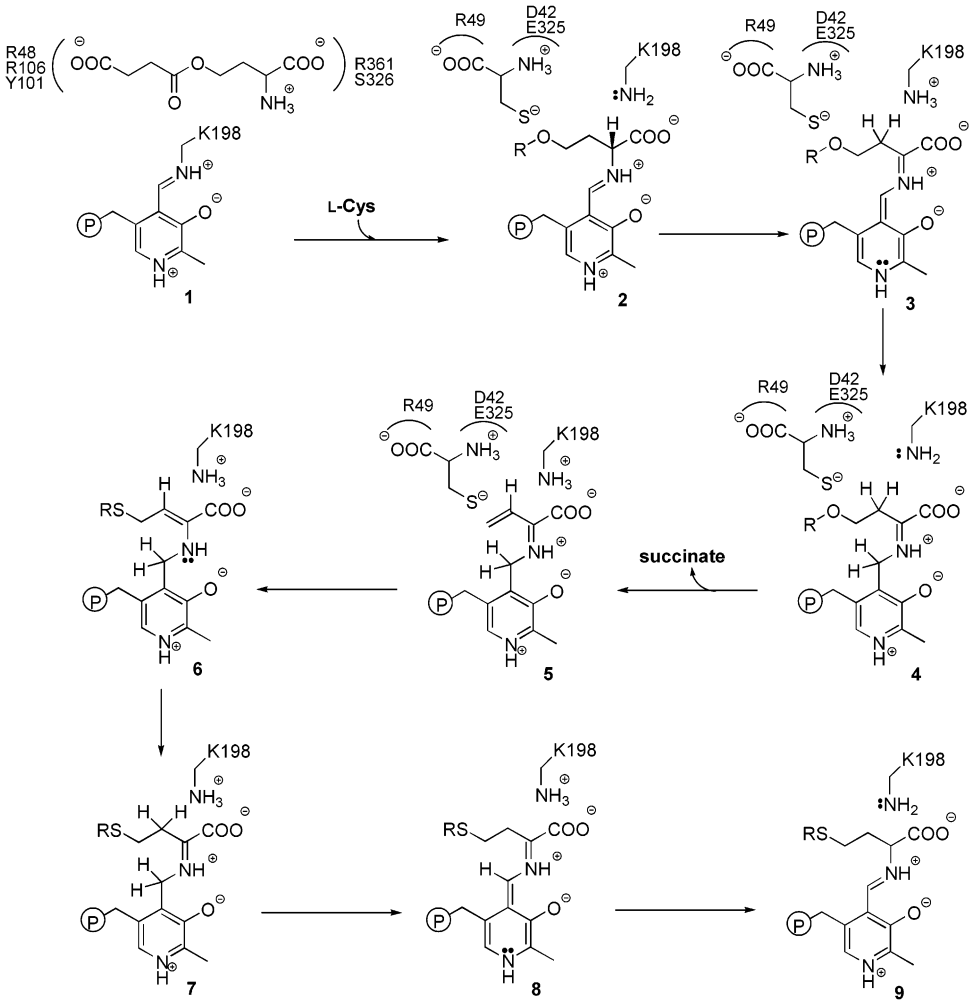

[a] The structure of **5** is that proposed by Brzovic *et al.* (*12*), and the assignment of active site residues is based on the eCGS crystal structure (*1*).

Scheme 2: L-Cysteine and L-Methionine Metabolism in *E. coli* (*28*)

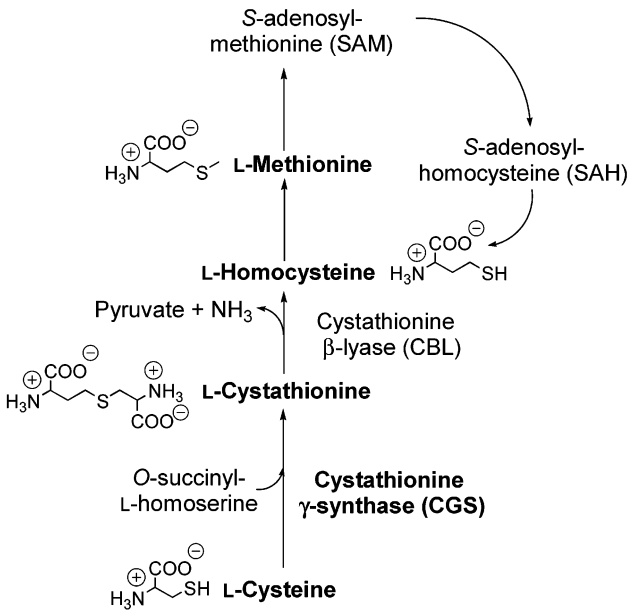

insight into the chemical mechanism of this reaction. The kinetic mechanism for the replacement reaction has been interpreted in terms of a ping-pong model with succinate elimination preceding L-Cys association (*11*). However, the steady-state mechanism has not been thoroughly investigated because of the lack of suitable assays. The ratio of the reported k_{cat} values for the replacement and elimination reactions is only 1.5 (*11*), which is surprising, given the *in vivo* role of eCGS in transsulfuration. Here we describe novel continuous assays for the elimination and substitution reactions of CGS, which are employed to characterize the steady-state kinetics of eCGS. The kinetic mechanism is shown to be ordered at L-Cys concentrations greater than K_m^{L-Cys}. The pH dependencies of the elimination and replacement reactions are described.

EXPERIMENTAL PROCEDURES

Reagents. L-Cys was purchased from Fluka. L-Lactate dehydrogenase (LDH) and *O*-succinyl-L-homoserine (L-OSHS) were Sigma products. Protease inhibitor (Complete EDTA-free) tablets were from Roche. DEAE-Sepharose fast-flow resin was purchased from Amersham Pharmacia Biotech. Toyopearl butyl-650M resin was from TosoHaas. Ni−NTA resin was a Qiagen product. 5,5′-Dithiobis(2-nitrobenzoic acid) (DTNB) was from Pierce. Isopropyl β-D-thiogalactopyranoside (IPTG) was from CalBiochem. His-tagged eCBL was expressed and purified as described previously (*14*).

His Tagging, Expression, and Purification of D-2-Hydroxyisocaproate Dehydrogenase (HO-HxoDH). The gene

Scheme 3: Mechanism of the eCGS γ-Elimination Reaction[a]

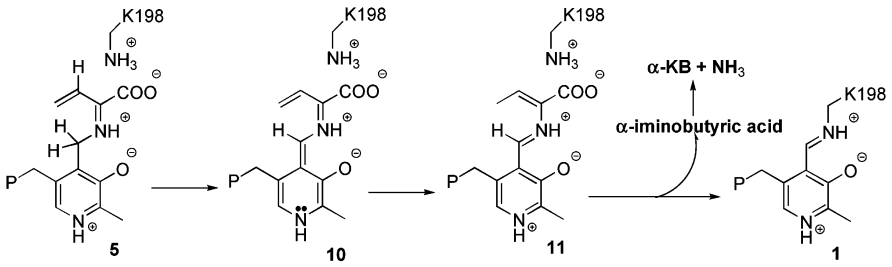

[a] The reaction mechanism is that proposed by Brzovic *et al.* (*12*). Structures **1** and **5** are from Scheme 1.

encoding HO-HxoDH was subcloned from the plasmid pGIN113 (*15*) with HO-HxoDH-specific primers designed to introduce restriction sites and a C-terminal six-His tag: 5′-TAT TAA CCA *TG*G CTA AAA TTG CCA TGT ATA ATG TC-3′ and 5′-TCC AAT GCA TTG GCT GCA GTT AAT GGT GGT GAT GGT GGT GCA GGT TAA CGA TGC TTC TTG GCC GG-3′ (restriction sites are underlined, and the ATG start codon is in italics). The His-tagged HO-HxoDH gene was introduced into the pTrc-99a vector (Amersham Pharmacia Biotech) and transformed into *E. coli* strain DH10B (Gibco BRL) *via* electroporation (Gene Pulser, Bio-Rad).

Three liters of LB medium (4 × 750 mL in 2.8 L baffled Fernbach flasks) was warmed at 37 °C for 3 h followed by addition of ampicillin to a final concentration of 100 μg/mL and inoculation (1:50) with an overnight pTrc-99a/HO-HxoDH culture in *E. coli* DH10B in LB (100 μg/mL ampicillin). IPTG was added to a final concentration of 0.1 mM when the OD_{600} reached 0.5, and the cells were incubated at 30 °C for a further 6 h. The harvested cell pellet was suspended in 30 mL of buffer A [50 mM potassium phosphate (pH 7.8), 10 mM β-mercaptoethanol, and 10 mM imidazole] containing one Complete EDTA-free tablet (Roche) and 20 μg/mL DNAse I. The cells were disrupted by incubation with 1 mg/mL lysozyme on ice for 20 min followed by repeated (8 × 30 s) cycles in a Bead Beater (Biospec Products). The lysate was centrifuged, the supernatant loaded onto a 1.5 × 10 cm column of Ni−NTA resin, and the column washed with 200 mL of buffer A. The enzyme was eluted with a 400 mL linear gradient of 10 to 400 mM imidazole in buffer A. The HO-HxoDH-containing fractions were pooled, concentrated, and dialyzed against storage buffer [50 mM triethanolamine (pH 6.5)]. Approximately 50 mg of ≥95% pure HO-HxoDH was obtained from the 3 L culture.

Cloning, Expression, and Purification of eCGS. The *metB* gene encoding eCGS (*16*) was PCR amplified from the genomic DNA of *E. coli* JM103 with the eCGS-specific primers 5′-GGG TAC TGA CCG TAA ACC CGC ATA GTT TA-3′ and 5′-CAC CGA TTT GTG TCG CGG AAT AGT CGG AAC-3′. Restriction sites were subsequently introduced by PCR with the primers 5′-G GAA CTT CAT C*CC ATG* GCG CGT AAA CAG G-3′ and 5′-CCT TGT TGA TTA GGT ACC GCA GAC ATC AGA CGT-3′ (restriction sites are underlined, and the ATG start codon is in italics). The eCGS gene was introduced into the pTrc-99a vector (Amersham Pharmacia Biotech) and transformed into *E. coli* strain DH10B as described above.

A 4.5 L (6 × 750 mL in 2.8 L baffled Fernbach flasks) pTrc-99a/eCGS culture in *E. coli* DH10B was grown and harvested as described above for HO-HxoDH. The harvested cell pellet was suspended in 40 mL of buffer B [50 mM potassium phosphate (pH 7.2), 1 mM EDTA, and 20 μM PLP] containing one Complete EDTA-free tablet (Roche) and 20 μg/mL DNAse I. Cells were disrupted as described above. The lysate was centrifuged, ammonium sulfate added to the supernatant to 30% saturation, and the resulting solution loaded onto a 2.5 × 10 cm column of Toyopearl butyl-650M resin (TosoHaas) equilibrated with buffer B containing 30% ammonium sulfate. The column was washed with 400 mL of buffer B containing 30% ammonium sulfate, and the enzyme was eluted with a 400 mL linear gradient of 30 to 0% ammonium sulfate in buffer B. The eCGS-containing fractions were pooled, concentrated, dialyzed against buffer B to remove the ammonium sulfate, and loaded onto a 2.5 × 10 cm column of DEAE-Sepharose resin (Amersham Pharmacia Biotech). The column was washed with 400 mL of buffer B, and the enzyme was eluted with a 400 mL linear gradient of 0 to 500 mM NaCl in buffer B. The purified protein was concentrated and dialyzed against buffer B. Approximately 90 mg of ≥95% pure eCGS was obtained from the 4.5 L culture.

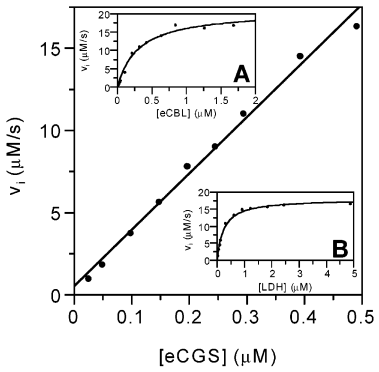

FIGURE 1: Dependence of the rate of NADH oxidation upon eCGS, eCBL (inset A), and LDH (inset B) concentration in the coupled eCBL/LDH assay. Reactions were carried out in 1 mL volumes at 25 °C, and the rates were monitored at 340 nm. Conditions: 50 mM Tris (pH 7.8), 200 μM NADH, 20 μM PLP, 20 mM L-OSHS, and 0.5 mM L-Cys with 0.025−0.49 μM eCGS, 0.84 μM eCBL, and 1.8 μM LDH (main panel), with 0.25 μM eCGS, 0.011−1.7 μM eCBL, and 1.8 μM LDH (inset A), or with 0.25 μM eCGS, 0.84 μM eCBL, and 0.031−4.9 μM LDH (inset B).

Enzyme Assays. CGS activity was measured in a total volume of 150 μL at 25 °C on an HP 8453 UV−vis spectrophotometer. The assay buffer contained 50 mM Tris (pH 7.8) and 20 μM PLP. Samples were equilibrated at 25 °C, and a background rate was recorded prior to initiation of the reaction. Data were fitted by nonlinear regression with the program SAS (SAS Institute, Cary, NC).

Scheme 4: Continuous Coupled Enzyme Assays Developed for CGS[a]

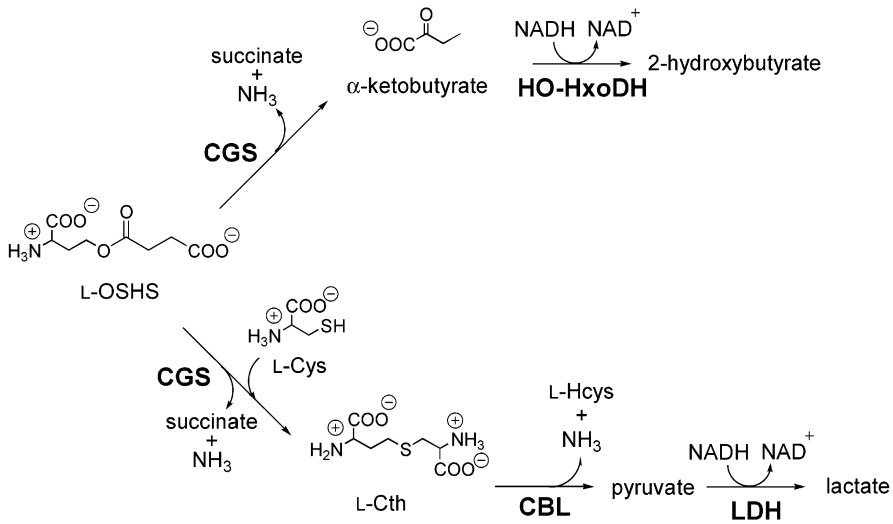

[a] Elimination of succinate from L-OSHS yields NH_3 and α-KB from α-iminobutyric acid. The coupling enzyme, HO-HxoDH, reduces α-KB to 2-hydroxybutyrate with NADH. CGS also catalyzes the replacement of the γ-succinate group of L-OSHS with L-Cys to form L-Cth. L-Cth is converted to L-Hcys, NH_3, and pyruvate by CBL, and the oxidation of the latter to lactate by LDH is monitored by NADH oxidation.

CGS Elimination Reaction Assay. Reactions were carried out in assay buffer containing 0.1−10 mM L-OSHS, 200 μM NADH, and 21 μM HO-HxoDH. The latter concentration is sufficient for coupling under these conditions. Reactions were initiated by the addition of 9.3 μM eCGS, and the conversion of NADH to NAD^+ was monitored at 340 nm ($\Delta\epsilon_{340} = 6200\ M^{-1}\ cm^{-1}$). Values for k_{catE} and K_{mE}^{L-OSHS} were obtained by fitting the data to the Michaelis−Menten equation, and k_{catE}/K_{mE}^{L-OSHS} was obtained independently from eq 1.

$$\frac{v}{[E]} = \frac{(k_{catE}/K_{mE}^{L-OSHS})[\text{L-OSHS}]}{1 + [\text{L-OSHS}]/K_{mE}^{L-OSHS}} \quad (1)$$

CGS Replacement Reaction Assay. eCBL and LDH concentrations of 0.84 and 1.8 μM, respectively, were selected for the CGS assay because each is in the plateau region of the coupling enzymes (Figure 1, insets A and B) for the range of eCGS concentrations that were assayed. Reactions were carried out in assay buffer containing 200 μM NADH, 1.8 μM LDH, 0.84 μM eCBL, 0.023−1.35 mM L-Cys, and 0.1−22.5 mM L-OSHS. They were initiated by the addition of 0.025−0.25 μM eCGS and monitored as described above. The rate of NADH oxidation in the CBL/LDH continuous assay is linearly dependent on the eCGS concentration over the specified range (Figure 1). The concentration of the L-Cys stock solution was determined with DTNB (*17*).

Single-Turnover Measurements. The reactions of 2.5 μM eCGS with 10 mM L-OSHS and 0−10 mM L-Cys in 50 mM Tris (pH 7.8) at 25 °C were monitored at 300 nm during the first 0.2 s of the reaction with a stopped-flow spectrophotometer (Applied Photophysics Ltd., SF.17MV), and the data were fitted to eq 2.

$$A_{320} = A_{max} - \Delta A e^{-k_{obs}t} \quad (2)$$

The resulting k_{obs} values were plotted *versus* L-Cys concentration.

Evaluation of the pH Dependence of the Kinetic Parameters of eCGS. The pH dependencies of the kinetic parameters for the eCGS elimination and replacement reactions were determined with the continuous HO-HxoDH and CBL/LDH assays, respectively. A three-component buffer, comprised of 50 mM MOPS ($pK_a = 7.2$), 50 mM Bicine ($pK_a = 8.3$), and 50 mM proline ($pK_a = 10.7$), was employed to keep the ionic strength constant ($I_c = 0.28$) (*18*, *19*). The kinetic measurements for the elimination reaction were carried out from pH 6.1 to 9.0 in the presence of 0.1−20 mM L-OSHS, 20 μM PLP, 200 μM NADH, 21 μM HO-HxoDH, and 9.3 μM eCGS. The kinetic measurements for the replacement reaction were carried out from pH 6.6 to 9.4 in the presence of 0.05−1.0 mM (0.05−2.5 mM at pH ≥8.8) L-Cys, 0.625−21.2 mM L-OSHS, 20 μM PLP, 200 μM NADH, 0.7−14 μM eCBL, 4.1 μM LDH, and 0.25−2.5 μM eCGS. The required concentration of eCBL increased with pH, and the optimal concentrations of both coupling enzymes were determined at each pH. The pH dependence of k_{cat} was fitted to eq 3, and that of k_{cat}/K_m^{L-OSHS} was fitted to the bell-shaped curve described by eq 4:

$$k_{cat} = \frac{(k_{cat})_{max}}{1 + 10^{pK_{a1}-pH}} \quad (3)$$

$$k_{cat}/K_m^{L-OSHS} = \frac{(k_{cat}/K_m^{L-OSHS})_{max}}{1 + 10^{pK_{a1}-pH} + 10^{pH-pK_{a2}}} \quad (4)$$

where $(k_{cat})_{max}$ and $(k_{cat}/K_m^{L-OSHS})_{max}$ are the upper limit values for the kinetic parameters.

Spectrophotometric Titration of the eCGS Internal Aldimine. The internal aldimine of eCGS was titrated *versus* pH with 20 μM enzyme in 5 mM TAPS ($pK_a = 8.4$; pH 6.70) containing 0.5 M KCl as a starting point. The pH was increased by successive additions of 0.5 M AMPSO (pH 10.6; $pK_a = 9.0$) at pH <9.0, 0.5 M CAPS (pH 11.5; $pK_a = 10.4$) between pH 9.0 and 10.5, and 1.0 M NaOH at pH >10.5. The enzyme solution was drawn through a 0.2 μm filter to reduce light scattering from the precipitate, and the

Table 1: Kinetic Parameters for the eCGS Replacement and Elimination Reactions[a]

	modified ping-pong mechanism[b,c]	ordered mechanism[b,d]	ref *11*[f]
	O-Succinyl-L-homoserine + L-Cysteine → Succinate + L-Cystathionine		
k_{catR} (s^{-1})	121 ± 5	117 ± 5	11.7
K_{mR}^{L-OSHS} (mM)	2.5 ± 0.5	1.2 ± 0.7	1.0
K_{mR}^{L-Cys} (mM)	0.11 ± 0.01	0.10 ± 0.01	0.05
K_{iR}^{L-Cys} (mM)	0.33 ± 0.09	0.2 ± 0.1	
K_{iR}^{L-OSHS} (mM)		2.0 ± 0.5	
k_{catR}/K_{mR}^{L-OSHS} (M^{-1} s^{-1})[d]	(4.9 ± 0.9) × 10^4	9.8 × 10^4	1.17 × 10^4
k_{catR}/K_{mR}^{L-Cys} (M^{-1} s^{-1})	(1.06 ± 0.07) × 10^6	(1.20 ± 0.01) × 10^6	2.34 × 10^5
	O-Succinyl-L-homoserine → Succinate + Pyruvate + NH_3		
k_{catE} (s^{-1})	1.80 ± 0.05[e]		7.7
K_{mE}^{L-OSHS} (mM)	1.3 ± 0.1[e]		0.33
k_{catE}/K_{mE}^{L-OSHS} (M^{-1} s^{-1})	1350 ± 90[e]		2.3 × 10^4

[a] The subscripts E and R denote kinetic parameters of the elimination and replacement reactions, respectively. The kinetic parameters are expressed per subunit. [b] Kinetic measurements were carried out in 50 mM Tris (pH 7.8) containing 20 μM PLP, 0.84 μM eCBL, 1.8 μM LDH, 200 μM NADH, 0.023−1.35 mM L-Cys, 0.1−22.5 mM L-OSHS, and 0.025−0.25 μM eCGS at 25 °C. [c] Data were fitted to eqs 7−9. [d] Data were fitted to eq 10. [e] Kinetic measurements were carried out in 50 mM Tris (pH 7.8), 20 μM PLP, 21 μM HO-HxoDH, 200 μM NADH, 0.1−10 mM L-OSHS, and 9.3 μM eCGS at 25 °C. Data were fitted to the Michaelis−Menten equation and to eq 1. [f] In the replacement reaction protocol of Holbrook *et al.* (*11*), eCGS was preincubated with L-Cys in 50 mM KPP_i (pH 7.8) containing 10 mM DTT. Reactions were initiated by the addition of [^{14}C]-L-OSHS, the mixtures incubated at 25 °C for 10−30 min, and the reactions stopped by the addition of 9 volumes of 3% perchloric acid. [^{14}C]-L-Cth was isolated with Dowex 50-X8 resin prior to quantitation.

pH of the solution was determined prior to each absorbance measurement. Spectra were recorded on an HP 8453 UV−vis spectrophotometer. The data recorded at 390 and 423 nm were fitted to eqs 5 and 6, respectively:

$$A = \frac{A_1 - A_2}{1 + 10^{pH - pK_{spec}}} + A_2 \quad (5)$$

$$A = \frac{A_1 - A_2}{1 + 10^{pK_{spec} - pH}} + A_2 \quad (6)$$

where A_1 and A_2 are the high and low absorbance limits at a particular wavelength, respectively.

RESULTS

A Continuous Assay for the CGS Elimination Reaction. The HO-HxoDH-catalyzed reduction of α-KB provides a suitable coupling reaction for the CGS-catalyzed hydrolysis of L-OSHS to succinate, α-KB, and NH_3, allowing the formation of α-KB to be monitored continuously in the elimination reaction (Scheme 4). The $k_{cat}/K_m^{\alpha-KB}$ of 1.6 × 10^4 M^{-1} s^{-1} (per subunit) for the reduction of α-KB to 2-hydroxybutyrate by HO-HxoDH, under eCGS assay conditions, is close to the reported value of 2.8 × 10^4 M^{-1} s^{-1} at pH 7.5 (*15*). In contrast, the $k_{cat}/K_m^{\alpha-KB}$ of LDH (1800 M^{-1} s^{-1} under eCGS assay conditions), which has been employed as a coupling enzyme for the CGS elimination reaction (*7*), is 1 order of magnitude lower than the value of that parameter for HO-HxoDH. The rate of the elimination reaction was determined in Tris buffer as a function of L-OSHS concentration, and the Michaelis−Menten parameters are included in Table 1. The kinetic parameters for the elimination reaction were also determined in $NaPP_i$ buffer (k_{catE} = 5.49 ± 0.07 s^{-1} and K_{mE}^{L-OSHS} = 0.29 ± 0.02 mM, where the subscript E denotes kinetic parameters of the elimination reaction) since previous studies on both eCGS (*11*) and stCGS (*7*, *20*) were carried out in pyrophosphate buffer. The k_{catE}/K_{mE}^{L-OSHS} is 1 order of magnitude higher in $NaPP_i$ [(1.2 ± 0.1) × 10^4 M^{-1} s^{-1}] than in Tris buffer [1350 ± 90 M^{-1} s^{-1} (Table 1)].

A Continuous Assay for the CGS Replacement Reaction. The formation of L-Cth is monitored continuously with the coupling enzymes eCBL (k_{cat}/K_m^{L-Cth} = 1.3 × 10^5 M^{-1} s^{-1}) and LDH (k_{cat}/K_m^{Pyr} = 1.1 × 10^5 M^{-1} s^{-1} under current assay conditions) in the CGS-catalyzed displacement of succinate from L-OSHS by L-Cys (Scheme 4). The kinetic parameters determined for the eCGS substitution reaction are presented in Table 1.

Kinetic Mechanism of eCGS. The β,γ-unsaturated ketimine intermediate formed by eCGS from L-OSHS decomposes to NH_3 and α-KB, returning the enzyme to the internal aldimine (*12*). Therefore, the eCGS mechanism cannot be reduced to a simple ping-pong mechanism. Sample data for the replacement reaction are shown in Figure 2. The decrease in v_i/[E] at elevated L-Cys concentrations is indicative of substrate inhibition (Figure 2B). Equations 7−9 were derived for the model shown in Scheme 5, which incorporates substrate inhibition by L-Cys into a modified ping-pong mechanism where the β,γ-unsaturated ketimine intermediate can either decay to release NH_3 and α-KB or react with L-Cys.

$$\frac{v}{[E]} = \left(k_{catE}[\text{L-OSHS}] + \frac{k_{catRp}}{K_{mRp}^{L-Cys}}[\text{L-OSHS}][\text{L-Cys}]\right) \Big/ \left[K_{mE}^{L-OSHS} + [\text{L-OSHS}] + \frac{K_{mRp}^{L-OSHS}}{K_{mRp}^{L-Cys}}\left(1 + \frac{[\text{L-Cys}]}{K_{iRp}^{L-Cys}}\right)[\text{L-Cys}] + \frac{1}{K_{mRp}^{L-Cys}}[\text{L-OSHS}][\text{L-Cys}]\right] \quad (7)$$

K_{iRp}^{L-Cys} is the dissociation constant for the E−L-Cys complex, where the subscripts R and p refer to the replacement reaction and ping-pong model, respectively. The data obtained for eCGS in the eCBL/LDH coupled assay (Figure 2) were fitted to eq 7 to obtain k_{catE} (3 ± 5 s^{-1}) and K_{mE}^{L-OSHS} (4 ± 1 mM). Despite the large error in these values, they are close to those determined directly in the absence of L-Cys (Table 1), showing that L-Cys does not significantly influence the rate of the elimination reaction. The values of k_{catE} and K_{mE}^{L-OSHS} determined *via* the elimination assay were subsequently substituted into eqs 7−9 to reduce the number of kinetic parameters to be determined, and the resulting fitted

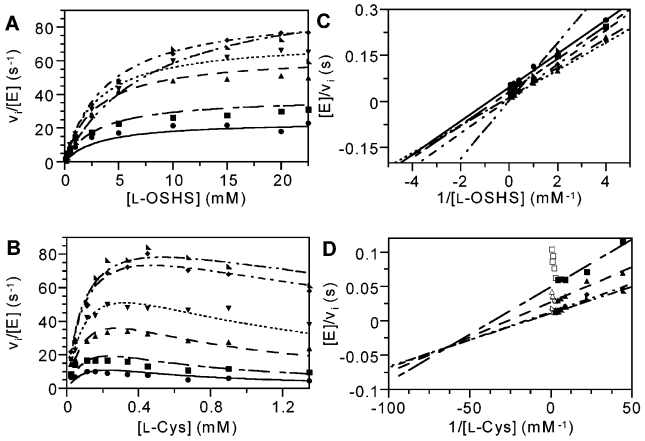

FIGURE 2: Steady-state initial velocity kinetics for eCGS showing the dependence of the γ-replacement reaction on L-OSHS and L-Cys concentrations. (A) Effect of L-OSHS concentration at fixed concentrations of L-Cys [0.023 (●), 0.045 (■), 0.11 (▲), 0.16 (▼), 0.34 (◆), and 0.90 mM (tilted triangles)]. (B) Effect of L-Cys concentration at fixed concentrations of L-OSHS [0.5 (●), 1.0 (■), 2.5 (▲), 5.0, (▼), 15 (◆), and 20 mM (tilted triangles)]. The lines represent the fit of the entire data set to eq 10. The fitted parameters are given in Table 1. Conditions: 0.84 μM eCBL, 1.8 μM LDH, 0.023−1.35 mM L-Cys, and 0.1−22.5 mM L-OSHS. The reactions were initiated by addition of eCGS (0.025−0.25 μM). Other conditions were as described in the legend of Figure 1. (C) Double-reciprocal plots of the data for 1/[L-OSHS]. (D) Double-reciprocal plots of the data for 1/[L-Cys], in which only the data at [L-Cys] < 0.34 mM (filled symbols) were fitted, as substrate inhibition by L-Cys results in curvature at [L-Cys] > 0.34 mM (empty symbols).

Scheme 5: Hybrid Ordered/Modified Ping-Pong Kinetic Mechanism Describing the eCGS-Catalyzed Elimination and Substitution Reactions[a]

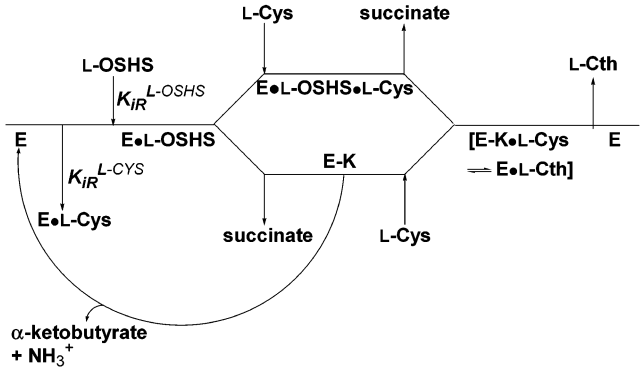

[a] L-OSHS associates with the enzyme to form the external aldimine (E−L-OSHS). Succinate is eliminated to form the β,γ-unsaturated ketimine complex (E−K) (*12*). In the absence of L-Cys, this species slowly decomposes to NH_3, α-KB, and the internal aldimine form of the enzyme via the elimination reaction. L-Cys, when present at saturating concentrations, reacts 65-fold more rapidly with E−K than α-iminobutyric acid is eliminated. When [L-Cys] > K_{mR}^{L-Cys}, the replacement reaction proceeds via an ordered mechanism and L-Cys binds to the E−L-OSHS complex prior to the release of succinate. When [L-Cys] < K_{mR}^{L-Cys}, the mechanism is ping-pong and succinate is eliminated prior to binding of L-Cys. Substrate inhibition (K_{iR}^{L-Cys}) is due to competition by L-Cys with L-OSHS for the free enzyme (E), to form a nonproductive E−L-Cys complex.

parameters for the replacement reaction are presented in Table 1. The terms in eq 7 were multiplied by K_{mRp}^{L-Cys}, yielding eq 8, to which the data were fitted to obtain k_{catRp} (121 ± 5 s^{-1}), K_{mRp}^{L-OSHS} (2.5 ± 0.5 mM), and K_{mRp}^{L-Cys} (0.11 ± 0.01 mM).

$$\frac{v}{[E]} = (k_{catE}K_{mRp}^{L-Cys}[\text{L-OSHS}] + k_{catRp}[\text{L-OSHS}][\text{L-Cys}])/\left[K_{mE}^{L-OSHS}K_{mRp}^{L-Cys} + K_{mRp}^{L-Cys}[\text{L-OSHS}] + K_{mRp}^{L-OSHS}\left(1 + \frac{[\text{L-Cys}]}{K_{iRp}^{L-Cys}}\right)[\text{L-Cys}] + [\text{L-OSHS}][\text{L-Cys}]\right] \quad (8)$$

The terms in eq 8 were divided by K_{mRp}^{L-OSHS} to give eq 9, from which $k_{catRp}/K_{mRp}^{L-OSHS}$ [(4.9 ± 0.9) × 10^4 M^{-1} s^{-1}] was obtained.

$$\frac{v}{[E]} = \left(\frac{k_{catE}K_{mRp}^{L-Cys}}{K_{mRp}^{L-OSHS}}[\text{L-OSHS}] + \frac{k_{catRp}}{K_{mRp}^{L-OSHS}}[\text{L-OSHS}][\text{L-Cys}]\right)/\left(\frac{K_{mE}^{L-OSHS}K_{mRp}^{L-Cys}}{K_{mRp}^{L-OSHS}} + \frac{K_{mRp}^{L-Cys}}{K_{mRp}^{L-OSHS}}[\text{L-OSHS}] + \left(1 + \frac{[\text{L-Cys}]}{K_{iRp}^{L-Cys}}\right)[\text{L-Cys}] + \frac{1}{K_{mRp}^{L-OSHS}}[\text{L-OSHS}][\text{L-Cys}]\right) \quad (9)$$

The 36-fold difference between $k_{catRp}/K_{mRp}^{L-OSHS}$ and k_{catE}/K_{mE}^{L-OSHS} (1350 ± 90 M^{-1} s^{-1}) indicates that the replacement reaction is activated by L-Cys. Therefore, eCGS does not follow a ping-pong mechanism. In addition, despite the complication of eCGS double-reciprocal plots by L-Cys substrate inhibition, it is apparent that only at L-Cys concentrations that are lower than K_{mR}^{L-Cys} are the parallel lines diagnostic of a ping-pong mechanism observed (Figure 2C). At L-Cys concentrations that are greater than K_{mR}^{L-Cys}, the lines intersecting to the left of the *y*-axis, typical of an ordered mechanism, are observed, and at L-Cys concentrations that are greater than K_{iR}^{L-Cys}, the intersection shifts to the *y*-axis, because of substrate inhibition. The double-reciprocal plot for varying concentrations of L-Cys (Figure 2D) shows that as the L-OSHS concentration is increased the lines intersect to the left of the *y*-axis. The increase in the rate of formation of the 300 nm absorbing species (**4** in Scheme 1) with increasing L-Cys concentrations, up to 0.05 mM, also demonstrates that the eCGS mechanism is not ping-pong (Figure 3). Therefore, the data were also fitted to an ordered mechanism (eq 10), and the resulting kinetic parameters are presented in Table 1.

$$\frac{v}{[E]} = (k_{catR}[\text{L-OSHS}][\text{L-Cys}])/\left[K_{iR}^{L-OSHS}K_{mR}^{L-Cys}\left(1 + \frac{[\text{L-Cys}]}{K_{iR}^{L-Cys}}\right) + K_{mR}^{L-Cys}[\text{L-OSHS}] + K_{mR}^{L-OSHS}[\text{L-Cys}]\left(1 + \frac{[\text{L-Cys}]}{K_{iR}^{L-Cys}}\right) + [\text{L-OSHS}][\text{L-Cys}]\right] \quad (10)$$

K_{iR}^{L-OSHS} is the dissociation constant for the E−L-OSHS complex. The only parameters whose values are significantly changed are K_{mR}^{L-OSHS} and K_{iR}^{L-Cys} (from K_{mRp}^{L-OSHS} and

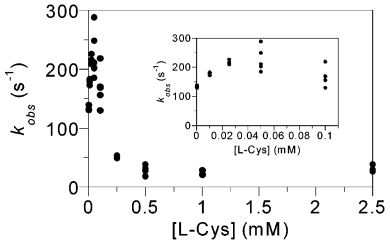

FIGURE 3: Effect of L-Cys on the rate of formation of the 300 nm absorbing species (**4**, Scheme 1). eCGS (2.5 μM) was reacted with 10 mM L-OSHS and 0−10 mM L-Cys in 50 mM Tris (pH 7.8) at 25 °C. Data were collected at 300 nm for 0.2 s with a stopped-flow spectrophotometer (see Experimental Procedures) and were fitted to eq 2 to obtain k_{obs}, which is plotted *vs* [L-Cys]. The inset shows the data for 0−0.1 mM L-Cys with an expanded concentration scale.

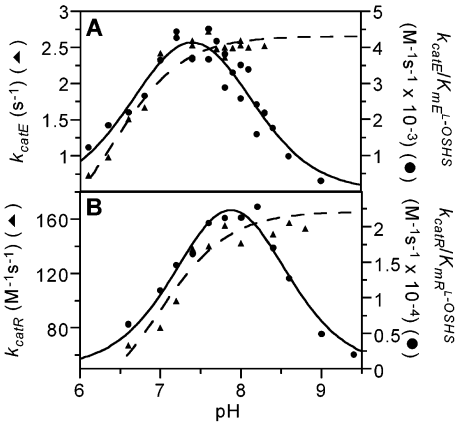

FIGURE 4: pH dependence of k_{cat} and k_{cat}/K_m^{L-OSHS} for the eCGS-catalyzed elimination and replacement reactions. (A) k_{catE} (▲) and k_{catE}/K_{mE}^{L-OSHS} (●) *vs* pH for the eCGS-catalyzed hydrolysis of L-OSHS to succinate, α-KB, and NH_3, monitored with the HO-HxoDH assay. Reaction conditions: 50 mM MBP (50 mM MOPS, 50 mM Bicine, and 50 mM proline), 20 μM PLP, 200 μM NADH, 21 μM HO-HxoDH, 0.1−20 mM L-OSHS, and 9.3 μM eCGS. The highest L-OSHS concentration that was used (20 mM) does not saturate at pH >8.6; thus, k_{catE} could not be obtained at high pH, and the data were fitted only to eq 1 to obtain k_{catE}/K_{mE}^{L-OSHS}. (B) k_{catR} (▲) and k_{catR}/K_{mR}^{L-OSHS} (●) *vs* pH for the eCGS-catalyzed condensation of L-OSHS and L-Cys to L-Cth, monitored with the CBL/LDH assay. Reaction conditions: 50 mM MBP, 20 μM PLP, 200 μM NADH, 0.7−14 μM eCBL, 4.1 μM LDH, 0.05−1.0 mM L-Cys (0.05−2.5 mM at pH ≥8.8), 0.625−21.2 mM L-OSHS, and 0.25−2.5 μM eCGS. The lines represent the nonlinear regression fits of the k_{cat} *vs* pH profile to eq 3 and of the k_{cat}/K_m^{L-OSHS} *vs* pH profile to eq 4.

K_{iRp}^{L-Cys} in the ping-pong mechanism of eq 7), which are decreased from 2.5 ± 0.5 and 0.33 ± 0.09 mM, respectively, in the modified ping-pong mechanism to 1.2 ± 0.7 and 0.2 ± 0.1 mM, respectively, in the ordered mechanism (Table 1).

Although the values obtained for K_{mR}^{L-OSHS} (1.2 ± 0.7 mM) and K_{mR}^{L-Cys} (0.11 ± 0.01 mM) are within 1.2-fold of those reported (Table 1), k_{catR} [117 ± 5 s^{-1} (Table 1)] is 10-fold greater than the reported value of 11.7 s^{-1} for eCGS (*11*). In contrast to the elimination reaction, the effect of Tris *versus* $NaPP_i$ buffer (k_{catR} = 72 ± 2 s^{-1} and K_{mR}^{L-Cys} = 0.088 ± 0.007 mM at 20 mM L-OSHS) on the substitution reaction is negligible.

pH Dependence of eCGS Activity. Figure 4A shows the pH dependence of k_{catE} and k_{catE}/K_{mE}^{L-OSHS} for the eCGS-catalyzed hydrolysis of L-OSHS to succinate, α-KB, and NH_3. The fit of the k_{catE} data to eq 3 yielded a single pK_a value of 6.70 ± 0.07, while the k_{catE}/K_{mE}^{L-OSHS} data fitted to eq 4 gave a pK_{a1} of 6.8 ± 0.1, a pK_{a2} of 8.0 ± 0.1 (Table 2), and a pH optimum of 7.4.

Table 2: Parameters Determined from the pH Dependence of the eCGS Reactions

	limiting value	pK_{a1}	pK_{a2}
elimination k_{catE}[a,c] (s^{-1})	2.66 ± 0.06	6.70 ± 0.07	
elimination k_{catE}/K_{mE}^{L-OSHS} [a,c] (M^{-1} s^{-1})	6300 ± 700	6.8 ± 0.1	8.0 ± 0.1
substitution k_{catR}[b,c] (s^{-1})	166 ± 8	7.0 ± 0.3	
substitution k_{catR}/K_{mR}^{L-OSHS} [b,c] (M^{-1} s^{-1})	(3.8 ± 0.5) × 10^4	7.4 ± 0.1	8.3 ± 0.1
L-OSHS			9.71 ± 0.01[d]
eCGS internal aldimine			>10.5[d]

[a] Kinetic measurements for the elimination reaction were carried out from pH 6.1 to 9.0 in MBP buffer containing 0.1−20 mM L-OSHS, 20 μM PLP, 200 μM NADH, 21 μM HO-HxoDH, and 9.3 μM eCGS at 25 °C. [b] Kinetic measurements for the replacement reaction were carried out in MBP buffer (from pH 6.6 to 9.4) containing 0.05−1.0 mM (0.05−2.5 mM at pH ≥8.8) L-Cys, 0.625−21.2 mM L-OSHS, 20 μM PLP, 200 μM NADH, 0.7−14 μM eCBL, 4.1 μM LDH, and 0.25−2.5 μM eCGS. [c] Data for k_{cat} and k_{cat}/K_m^{L-OSHS} *vs* pH were fitted to eqs 3 and 4, respectively. [d] pK_a values determined by direct titration.

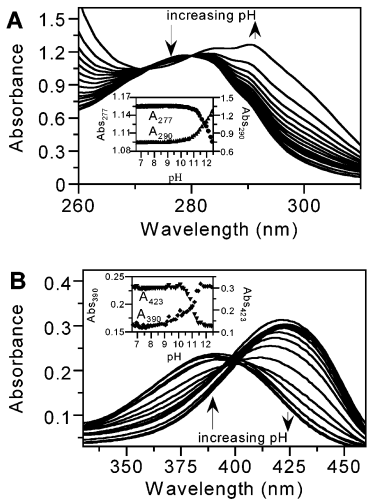

FIGURE 5: Spectrophotometric titration of 20 μM eCGS as a function of pH. (A inset) Absorbance at 277 (●) and 290 nm (▲) *vs* pH. (B inset) Absorbance at 390 (◆) and 423 nm (▼) *vs* pH. The spectra in the main part of the figure were recorded at pH 6.70, 7.53, 8.30, 9.45, 10.12, 10.37, 10.55, 10.65, 10.85, 11.01, 11.17, 11.32, 11.44, 11.62, 11.95, and 12.40.

The pH dependence of k_{catR} and k_{catR}/K_{mR}^{L-OSHS} for the eCGS-catalyzed condensation of L-OSHS and L-Cys to form L-Cth is shown in Figure 4B. The fit of the k_{catR} data to eq 3 demonstrated a single pK_a value of 7.0 ± 0.3, while the k_{catR}/K_{mR}^{L-OSHS} data fitted to eq 4 yielded a pK_{a1} of 7.4 ± 0.1, a pK_{a2} of 8.3 ± 0.1 (Table 2), and a pH optimum of 7.8.

The pK_a value of the α-NH_2 group of L-OSHS was determined by direct titration with NaOH to be 9.71 ± 0.01 at 25 °C. This value is 1.7 and 1.4 pH units higher than the pK_{a2} values of the k_{catE}/K_{mE}^{L-OSHS} and k_{catR}/K_{mR}^{L-OSHS} *versus* pH profiles, respectively (Table 2).

Spectrophotometric Titration of the eCGS Internal Aldimine. There is a shift in eCGS absorbance from 277 to 290 nm at pH >11 (Figure 5A) that likely reflects tyrosine ionization [pK_a = 10.13 (*21*, *22*)]. The 423 nm absorbance

of eCGS is lost at pH >10.5 (Figure 5B), within 0.5 pH unit of the tyrosine 277−290 nm shift. It is possible that PLP dissociates from the enzyme at high pH because the absorbance shifts to a maximum of 390 nm (Figure 5B), which is equal to that of free PLP (*23*).

DISCUSSION

The CGS-Catalyzed Elimination and Substitution Reactions Can Be Monitored Continuously. One of the products of the CGS elimination reaction, α-iminobutyric acid (Scheme 3), spontaneously hydrolyzes to NH_3 and α-KB (*24*). This reaction was previously monitored *via* an LDH coupled assay, where the α-KB is reduced to 2-oxobutyrate, with the concomitant oxidation of NADH (*7*). However, $k_{cat}/K_m^{\alpha-KB} = 1800\ M^{-1}\ s^{-1}$ (under eCGS assay conditions) for LDH, while the value of that parameter for HO-HxoDH is $1.6 \times 10^4\ M^{-1}\ s^{-1}$ under the same conditions; therefore, HO-HxoDH is a more efficient coupling enzyme for the elimination reaction of eCGS (Scheme 4). In comparison with the values reported by Holbrook *et al.* (*11*), the determined kinetic parameters for the eCGS-catalyzed elimination reaction in $NaPP_i$ buffer are reduced by less than 2-fold (1.4-,1.1-, and 1.9-fold lower for k_{catE}, K_{mE}^{L-OSHS}, and k_{catE}/K_{mE}^{L-OSHS}, respectively), while in Tris buffer, the k_{catE} is 3.1-fold lower, K_{mE}^{L-OSHS} is 4.5-fold greater, and k_{catE}/K_{mE}^{L-OSHS} is thus reduced by approximately 1 order of magnitude (Table 1). It is possible that pyrophosphate, but not Tris, is able to bind in place of L-Cys to induce a change in the active site conformation that facilitates elimination. For example, pyrophosphate might be a mimic of the carboxylate group of L-Cys, but Tris lacks a negatively charged group. Alternatively, Tris may inhibit the elimination reaction of eCGS.

Prior investigations of the CGS replacement reaction relied on end-point assays that monitor either production of [^{14}C]-L-Cth or consumption of L-Cys. The [^{14}C]-L-Cth assay requires the separation of the ^{14}C-labeled L-Cth product from the [^{14}C]-L-OSHS and L-Cys substrates followed by quantitation *via* scintillation counting (*11*, *25*). Although this assay is sensitive, it is laborious, involves significant sample handling that can lead to inaccuracy, and requires synthesis of the [^{14}C]-L-OSHS. The other assay that has been employed in the investigation of the CGS replacement reaction is a subtractive assay where the remaining L-Cys is quantitated with DTNB (*7*, *26*). Although this assay is less labor intensive than the [^{14}C]-L-Cth assay, it is less accurate due to the requirement for measuring small depletions in the L-Cys concentration. The limitations of the [^{14}C]-L-Cth and DTNB methods motivated the search for a continuous assay. Commonly available enzymes catalyzing reactions that capture nascent L-Cth that could be employed as coupling enzymes are limited to those of the transsulfuration pathway, CBL and CGL. CBL converts L-Cth to L-Hcys, NH_3, and pyruvate. The latter is conveniently monitored by the standard LDH assay (Scheme 4). Under eCGS assay conditions, both the k_{cat}/K_m^{L-Cth} of eCBL ($1.3 \times 10^5\ M^{-1}\ s^{-1}$) and the k_{cat}/K_m^{Pyr} of LDH ($1.1 \times 10^5\ M^{-1}\ s^{-1}$) are similar in magnitude to the k_{catR}/K_{mR}^{L-OSHS} ($4.9 \times 10^4\ M^{-1}\ s^{-1}$) for eCGS. Thus, a continuous assay is practical for eCGS. The concentration of LDH required, assuming a short lag period ($\tau = 4$ s), was estimated to be 2.3 μM [eq 11 (*14*, *27*)].

$$[LDH] = \frac{K_m^{Pyr}}{k_{cat}^{LDH}\tau} \quad (11)$$

This value was employed to calculate an eCBL concentration of 0.96 μM, that required to give an overall lag period of 12 s, *via* eq 12 (*14*, *27*).

$$[eCBL] = \frac{K_m^{L-Cth}/k_{cat}^{eCBL}}{\tau - (K_m^{Pyr}/k_{cat}^{LDH})[LDH]} \quad (12)$$

The calculated LDH and eCBL concentrations were subsequently optimized by independently varying the concentration of each (Figure 1). The results demonstrate the effectiveness of these enzymes for the continuous quantitation of L-Cth production by eCGS (Scheme 4).

eCGS Does Not Obey Ping-Pong Kinetics. The k_{cat}/K_m^{L-OSHS} describes the steps up to and including the first irreversible step, which is the release of succinate in both the elimination and replacement reactions. However, $k_{catRp}/K_{mRp}^{L-OSHS}$ is 36-fold greater than k_{catE}/K_{mE}^{L-OSHS} (Table 1), indicating that the elimination of succinate is activated by L-Cys in the replacement reaction and that eCGS does not obey the reported ping-pong mechanism (*11*). This conclusion is supported by the double-reciprocal plots (Figure 2C,D), which display intersecting rather than parallel lines typical of a ping-pong mechanism. Although the double-reciprocal plots are complicated by substrate inhibition by L-Cys, they suggest that eCGS actually has a hybrid mechanism (Scheme 5) that is ordered at L-Cys concentrations that are greater than K_{mR}^{L-Cys} and modified ping-pong, since the elimination reaction occurs from the unstable ketimine intermediate, at L-Cys concentrations that are lower than K_{mR}^{L-Cys}. The increase in the rate of formation of the 300 nm absorbing species [**4**, Scheme 1 (*12*)] from 134 ± 5 s^{-1} in the absence of L-Cys to 230 ± 40 s^{-1} at 0.05 mM L-Cys also supports an ordered mechanism. The pre-steady-state data indicate that the step that is accelerated by the presence of L-Cys is the elimination of succinate from the ketimine (**4**, Scheme 1), as this species is most likely the 300 nm absorbing species observed on reaction of eCGS with L-OSHS (Figure 3). The shift in the pH profiles between the elimination and replacement reactions (Figure 4), as well as the 10-fold increase in the k_{catE}/K_{mE}^{L-OSHS} in $NaPP_i$ *versus* Tris buffer, provides further support for an ordered rather than ping-pong mechanism. The requirement that both substrates be bound in a ternary complex, rather than L-Cys taking the place of the departed succinate, is consistent with the crystal structure of eCGS, as modeling has suggested that the carboxylate group of L-Cys is bound by Arg49, while that of the succinate moiety of L-OSHS interacts with Arg48, Arg106, and Tyr101 (*1*).

There is significant variation between the values of kinetic constants for the replacement reaction of eCGS presented in Table 1 ($k_{catR} = 117 \pm 5\ s^{-1}$, Tris, pH 7.8, 25 °C) and those reported by Holbrook *et al.* [$k_{catR} = 11.7\ s^{-1}$, KPP_i, pH 7.8, 25 °C, (*11*)]. There are a number of factors that likely contribute to this variation: (1) differences in the experimental conditions, i.e., Tris *versus* KPP_i buffer; (2) the assay employed, i.e., [^{14}C]-L-Cth discontinuous assay *versus* CBL/LDH continuous assay; and (3) the presence of inhibitory impurities present in the substrates, particularly the [^{14}C]-

L-OSHS. In addition, Holbrook *et al*. (*11*) did not report substrate inhibition by L-Cys, which could lead to a significant underestimation of k_{catR}. The ratio of k_{catR}/k_{catE} reported by Holbrook *et al*. (*11*) is only 1.5. This is unexpected given that the major role for this enzyme *in vivo* is to produce L-Cth in the transsulfuration pathway rather than to convert L-OSHS to succinate, α-KB, and NH_3 (*28*). Therefore, the newly determined values presented in Table 1 ($k_{catR}/k_{catE} = 65$) are more in line with the *in vivo* role of the *E. coli* enzyme.

In contrast to the kinetic parameters reported for eCGS (*11*), those for stCGS [$k_{catR} = 128\ s^{-1}$ (K_{mR}^{L-OSHS} not reported) in 50 mM KPP_i (pH 8.3) at 37 °C (*20*); $k_{catR} = 250\ s^{-1}$ and $k_{catR}/K_{mR}^{L-OSHS} = 6.25 \times 10^4\ M^{-1}\ s^{-1}$ in KPP_i (pH 8.2) at 37 °C (*7*)] are close to those obtained for eCGS in the investigation presented here. The variation is likely due to a combination of real differences between these homologous enzymes and changes in the experimental conditions, i.e., temperature (25 *vs* 37 °C) and pH (7.8 *vs* 8.2 and 8.3).

The continuous nature of the CBL/LDH assay eliminates L-Cth accumulation, and thus precludes product inhibition that might complicate parameter evaluation in discontinuous assays. However, product inhibition is not a significant factor for eCGS, in contrast to yeast cystathionine β-synthase (yCBS) (*14*), since the K_{mR}^{L-OSHS} (Table 1) determined with the continuous CBL/LDH assay is within 1.2-fold of the value determined for eCGS with the discontinuous [^{14}C]-L-Cth assay (*11*), indicating that L-Cth does not compete with L-OSHS for the free enzyme form of eCGS in the [^{14}C]-L-Cth assay. The decrease in the rate of the eCGS substitution reaction observed at elevated L-Cys concentrations (Figure 2B) is indicative of substrate inhibition ($K_{iR}^{L-Cys} = 0.2$ mM), which results from the binding of the substrate to the wrong form of the enzyme. Substrate inhibition by L-Cys is also observed in the reaction of eCGS with L-OSHS under pre-steady-state conditions (Figure 3). L-Cys is proposed to compete with L-OSHS for the free enzyme form of eCGS (Scheme 5). Substrate inhibition of eCGS by L-Cys has not been described previously.

pH Dependence of eCGS Activity and Spectral Properties of the Enzyme. The absorption spectrum of eCGS, at pH 7.0, exhibits a λ_{max} of 423 nm, which is diagnostic for the protonated form of the eCGS internal aldimine (*11*). Loss of this proton is accompanied by a shift in the maximum of the spectrum of the PLP aldimine to a λ_{max} of ~360 nm (*29*, *30*). The aldimine does titrate near neutral pH in some aminotransferases (*31*). However, the data depicted in Figure 5 show that the spectrum of the internal aldimine of eCGS is independent of pH from 6.7 to 10.5. The internal aldimine of stCGS also remains protonated between pH 5.5 and 9 (*8*). The decrease in absorbance at 423 nm and increase at 390 nm of eCGS at pH >10.5 (Figure 5B) are likely due to dissociation of PLP from the enzyme (*23*). This occurs concomitantly with the 277−290 nm shift (Figure 5A), which is indicative of tyrosine ionization (*21*, *22*). Therefore, it is likely that a conformational change in the protein is required to allow access of base to the aldimine. A similar interpretation of the pH dependence of the absorbance of the internal aldimine has been advanced for yCBS (*14*).

Three factors that have been identified as key determinants of the low pK_a of the internal aldimine of aspartate aminotransferase (AATase) from *E. coli* are (i) the salt bridge between the pyridinium nitrogen and an acidic residue [D222 (*32*)], (ii) the hydrogen bond between the phenoxylate oxygen of the PLP ring and Y225 (*31*), and (iii) the strain induced by the aldimine linkage to Lys258, which results in a destabilization of the planar conformation of the internal aldimine (*33*). These interactions decrease the electron density in the cofactor, resulting in a decrease in the pK_a of the internal aldimine. As in AATase, an aspartate residue forms a strong H-bond or salt bridge with the pyridinium nitrogen of the PLP ring in eCGS (D173); however, the phenoxylate oxygen of the eCGS PLP is weakly H-bonded to a water molecule (*1*). Thus, although the effect of imine−pyridine torsion in eCGS is unknown, the nature of the group interacting with the phenoxylate oxygen may be a greater factor than the salt bridge between D173 and the pyridinium nitrogen in determining the pK_a of the internal aldimine of eCGS.

The lack of suitable continuous assays may have discouraged detailed studies of the dependence of the kinetic parameters of eCGS on pH. However, a pH optimum of 8.2 was reported for the hydrolysis of L-OSHS to succinate, α-KB, and NH_3 by stCGS (*7*). The eCGS elimination reaction was reported to increase in activity to pH 8.8 and remain constant from pH 8.8 to 10.2 (*11*). A pH optimum of 7.8 has been reported for the replacement reaction of both eCGS (*11*) and stCGS (*7*). Both of these reports measured the specific activity at a single substrate concentration at each pH. Because of the lack of coincidence between the pK_a of the substrate (9.71 ± 0.01) or the internal aldimine (>10.5) and the kinetically determined pK_a values of k_{catE}/K_{mE}^{L-OSHS} ($pK_{a1} = 6.8 \pm 0.1$ and $pK_{a2} = 8.0 \pm 0.1$) and k_{catR}/K_{mR}^{L-OSHS} ($pK_{a1} = 7.4 \pm 0.1$ and $pK_{a2} = 8.3 \pm 0.1$), the latter must be assigned to enzyme groups other than the imino moiety of the internal aldimine.

The aldimine lysine (Lys198 of eCGS, which corresponds to Lys258 of *E. coli* AATase) and an active site tyrosine (Tyr101) were proposed as catalytic residues of eCGS (*1*). It was suggested that Tyr101 is involved in proton transfer during transaldimination and in protonation of the succinate leaving group, thus requiring that this residue be deprotonated at the optimal pH of the enzyme (*1*). The value of $9.8 \times 10^4\ M^{-1}\ s^{-1}$ for k_{catR}/K_{mR}^{L-OSHS} is lower than that expected for a diffusion-controlled reaction; therefore, the alternatives shown in eq 13 for the rates of formation of the Michaelis complex (eCGS·L-OSHS) or the external aldimine are kinetically indistinguishable, and no conclusions can be reached concerning the state of protonation of Tyr101 in the free enzyme.

$$\frac{d([eCGS][L\text{-}OSHS])}{dt} = k_2[R-NH_3^+][Y101-O^-] = k_2K[R-NH_2][Y101-OH] \quad (13)$$

K is the equilibrium constant between the prototropic bracketed entities on either side of eq 13. It would have a value of 0.16, assuming a pK_a of 10.5 for the OH group of Tyr101 and of 9.71 for the amino group of L-OSHS. Thus, the rate constants for the alternate pathways differ by a factor of only 6. It should also be noted that the second pK_a of succinic acid is 5.5 (*34*); thus, the leaving group does not

need to accept a proton at physiological pH. Therefore, the precise role of Tyr101 in proton transfer is at present unclear.

ACKNOWLEDGMENT

We acknowledge Dan Malashock, Andrew Eliot, and Edgar Deu for their assistance in interpretation of the kinetic data.

REFERENCES

1. Clausen, T., Huber, R., Prade, L., Wahl, M. C., and Messerschmidt, A. (1998) *EMBO J. 17*, 6827−6838.
2. Nagai, S., and Flavin, M. (1967) *J. Biol. Chem. 242*, 3884−3895.
3. Datko, A. H., Giovanelli, J., and Mudd, S. H. (1974) *J. Biol. Chem. 249*, 1139−1155.
4. Ono, B., Tanaka, K., Naito, K., Heike, C., Shinoda, S., Yamamoto, S., Ohmori, S., Oshima, T., and Toh-e, A. (1992) *J. Bacteriol. 174*, 3339−3347.
5. Steegborn, C., Messerschmidt, A., Laber, B., Streber, W., Huber, R., and Clausen, T. (1999) *J. Mol. Biol. 290*, 983−996.
6. Messerschmidt, A., Worbs, M., Steegborn, C., Wahl, M. C., Huber, R., Laber, B., and Clausen, T. (2003) *Biol. Chem. 384*, 373−386.
7. Kaplan, M. M., and Flavin, M. (1966) *J. Biol. Chem. 241*, 4463−4471.
8. Kaplan, M. M., and Flavin, M. (1966) *J. Biol. Chem. 241*, 5781−5789.
9. Guggenheim, S., and Flavin, M. (1969) *J. Biol. Chem. 244*, 3722−3727.
10. Guggenheim, S., and Flavin, M. (1971) *J. Biol. Chem. 246*, 3562−3568.
11. Holbrook, E. L., Greene, R. C., and Krueger, J. H. (1990) *Biochemistry 29*, 435−442.
12. Brzovic, P., Holbrook, E. L., Greene, R. C., and Dunn, M. F. (1990) *Biochemistry 29*, 442−451.
13. Guggenheim, S., and Flavin, M. (1969) *J. Biol. Chem. 244*, 6217−6227.
14. Aitken, S. M., and Kirsch, J. F. (2003) *Biochemistry 42*, 571−578.
15. Bernard, N., Johnsen, K., Ferain, T., Garmyn, D., Hols, P., Holbrook, J. J., and Delcour, J. (1994) *Eur. J. Biochem. 224*, 439−446.
16. Duchange, N., Zakin, M. M., Ferrara, P., Saint-Girons, I., Park, I., Tran, S. V., Py, M. C., and Cohen, G. N. (1983) *J. Biol. Chem. 258*, 14868−14871.
17. Ellman, G. L. (1959) *Arch. Biochem. Biophys. 82*, 70−77.
18. Jhee, K. H., McPhie, P., and Miles, E. W. (2000) *Biochemistry 39*, 10548−10556.
19. Peracchi, A., Bettati, S., Mozzarelli, A., Rossi, G. L., Miles, E. W., and Dunn, M. F. (1996) *Biochemistry 35*, 1872−1880.
20. Johnston, M., Jankowski, D., Marcotte, P., Tanaka, H., Esaki, N., Soda, K., and Walsh, C. (1979) *Biochemistry 18*, 4690−4701.
21. Voet, D., and Voet, J. G. (1990) *Biochemistry*, John Wiley and Sons, New York.
22. Edelhoch, H. (1967) *Biochemistry 6*, 1948−1954.
23. Metzler, C. M., Cahill, A., and Metzler, D. E. (1980) *J. Am. Chem. Soc. 102*, 6075−6082.
24. Posner, B. I., and Flavin, M. (1972) *J. Biol. Chem. 247*, 6412−6419.
25. Krueger, J. H., Johnson, J. R., and Greene, R. C. (1978) *J. Bacteriol. 133*, 1351−1357.
26. Kaplan, M. M., and Flavin, M. (1965) *Biochim. Biophys. Acta 104*, 390−396.
27. Easterby, J. S. (1973) *Biochim. Biophys. Acta 293*, 552−558.
28. Sekowska, A., Kung, H. F., and Danchin, A. (2000) *J. Mol. Microbiol. Biotechnol. 2*, 145−177.
29. Jenkins, W. T., and Sizer, I. W. (1957) *J. Am. Chem. Soc. 79*, 2655−2656.
30. Jenkins, W. T., Yphantis, D. A., and Sizer, I. W. (1959) *J. Biol. Chem. 234*, 51−57.
31. Goldberg, J. M., Swanson, R. V., Goodman, H. S., and Kirsch, J. F. (1991) *Biochemistry 30*, 305−312.
32. Yano, T., Kuramitsu, S., Tanase, S., Morino, Y., and Kagamiyama, H. (1992) *Biochemistry 31*, 5878−5887.
33. Hayashi, H., Mizuguchi, H., and Kagamiyama, H. (1998) *Biochemistry 37*, 15076−15085.
34. Sober, H. A. (1970) *CRC Handbook of Chemistry*, Chemical Rubber Co., Cleveland, OH.

BI035107O